EXPERIMENTAL INVESTIGATION OF ULTIMATE LOADS CARRIED BY FLAT, UNSTIFFENED PANELS UNDER COMBINED SHEAR AND COMPRESSION

Thesis

by

Wesley T. Butterworth

In Partial Fulfillment of the Requirements for the Degree of Master of Science in Aeronautical Engineering

California Institute of Technology

Pasadena, California

1938

Table of Contents

Index of Figures

Index of Photographs

Table of Notation

Symbol	Definition	Unit
P_{c_o}	Failure load in pure compression	lbs.
P_c	Applied compressive load in combined loading	lbs.
P_{s_o}	Failure load in pure shear	lbs.
P_s	Applied shear load in combined loading	lbs.
t	Thickness of sheet	inches
a	Length of panel measured parallel to compression axis	inches
b	Width of panel measured perpendicular to compression axis	inches
n	Exponent of P_s/P_{s_o} in Eq. 1, determined empirically	
η	Ratio of experimental ultimate load to calculated ultimate load in compression	

I. ACKNOWLEDGMENT

The author takes this opportunity to thank Dr. E. E. Sechler of the Guggenheim Aeronautical Laboratory, California Institute of Technology, for his careful direction of this research. He also wishes to thank W. L. Howland for his interested advice throughout the course of the investigation, and to thank Messrs. C. F. Friend and J. L. Nollan for their valuable assistance during the performance of experiments and the reduction of data.

II. SUMMARY

Four series of tests were made on flat, unstiffened panels under combined shear and compression loading for two thicknesses and two length over width ratios. In each case, the panels were carried to their ultimate loads. An empirical relation was developed for the variation of shear and compressive stresses of the form:

$$\left(\frac{P_c}{P_{c_o}}\right)+\left(\frac{P_s}{P_{s_o}}\right)^4 = 1$$

where: P_{c_o} = failure stress, pure compression,

P_{s_o} = failure stress, pure shear.

The above equation was found to hold for the entire range of thicknesses and length over width ratios investigated.

III. INTRODUCTION

In the stressed skin construction of modern airplanes, it becomes necessary, in many cases, to analyze certain panels which may act under the combined loadings of shear and compression. This situation is encountered, for instance, in the wings of such airplanes which are stressed by torsional moments while carrying lift loads. Again, rudder loads, eccentric to the fuselage, may introduce into that structure a combination of shear and compression.

With these problems in mind, the present investigation was begun. Throughout these tests 24ST duralumin sheet was used, since it was considered most representative of current structural materials in the aeronautics field. This sheet was cut into flat, unstiffened panels, with the grain of the material along the same axis for each test, leaving the curved and stiffened cases for future investigation. Two different thicknesses were tested, namely, 0.022" and 0.032", nominal size; likewise, two sizes of sheet were used for each thickness, giving length over breadth ratios of 2 and 3.

Several specimens were tested in shear alone, and in compression alone in order to determine the ultimate loads carried by a given panel under these single loads. The remainder of the tests were conducted by loading the

panel first with an appropriate compression load to be held constant, and then applying a shear load of increasing magnitude until the ultimate load of this combination was reached. For several tests, the order of application of load was reversed from the above to determine whether the sequence of loading had any noticeable effect. In each case split tubes were used for edge support of the sheet.

IV. EXPERIMENTAL PROCEDURE

(a) Apparatus

The panels were mounted in a compression testing-machine as shown in Fig. 1. The upper head, (a), of this machine is a ten-inch I-beam, and is bolted rigidly to the upright ten-inch channel sections. The lower head, (b), is also a ten-inch I-beam, pivoted on ball bearings at a seven-foot radius, with adjusting screws provided to align the lower head parallel to the upper. The horizontal motion of the lower head perpendicular to the plane of the sheet is less than 1% of the vertical displacement measured, hence was neglected.

The compressive loads were applied through a heavy steel ring of large diameter, part (c), Fig. 1. This ring gage was placed under the lower head of the machine, resting on a steel ball, and loaded through another steel ball by the adjusting bolt, (d), between the gage and the base of the machine. An Ames dial gage was arranged to measure the contraction of the ring under load. Two of such gages were employed, each being calibrated in a standard compression testing-machine several times. The calibration curves are shown in the Appendix.

The shear loading device, (e), consists of two steel straps, clamped together at the ends and initially bent away from each other in the center. Trunnions are provided

on each end of the instrument to eliminate bending about each of two axes; and it was found necessary to support the free end of the gage between rollers to eliminate the torque introduced by loading. Tightening the lead-screw nut against the uprights of the machine provided the shear load. Lateral contraction of the two straps at the center was measured by means of a sensitive Ames dial gage. The instrument was calibrated several times in a standard tensile-testing machine, and the resulting calibration curve is shown in the Appendix.

To eliminate the bending moment in the sheet introduced by applying the shear load to one end of the panel, a shaft carrying two roller bearings was installed directly above the lower angles between which the sheet was clamped. This shaft was fastened to the lower head of the machine, so that the roller bearings furnished a reaction moment to balance the applied moment due to shear loads.

The panels were clamped for testing between a pair of two-inch angles at each end. The upper set of angles was bolted to the upper head of the machine; while the lower set was bolted to a flat bar, separated from the lower head by steel rollers - to allow shear deflection. Guides were provided to confine the motion of the lower angles to the plane of the panel. The edges of the sheet were supported by means of tubes, split along an element, with bolts for clamping the split together.

(b) Testing Procedure

After accurately aligning the heads of the machine parallel to each other, the sheet was bolted between the angles at each end, taking care to locate the axis of the sheet along the compression axis. It was found necessary to fasten the sheet from the center outward at each end to avoid distortion of the sheet. Throughout all of these tests, the length of the panels was kept constant at 18 inches, measured from upper to lower angles.

The split tubes were attached securely to the edges of the sheet, allowing proper clearance between the ends of the tubes and the angles. In several cases, particularly on the thinner sheets, local failure at the corners where the edges were not supported was encountered. Therefore it became advisable to keep the length of this unsupported edge as short as consistent with reasonable clearance, adjusting during a test if necessary. These tubes also exhibited a tendency to spring off when the wave pattern of the sheet became quite deep. Hence, four turnbuckles were attached between the tubes to eliminate this condition, taking care not to introduce an edge-moment into the sheet when installing the turnbuckles.

For the pure compression tests, the shear loading device was disconnected and the sheet loaded by the ring gage previously described. Vertical deflection of the

sheet was measured by two Ames dial gages located on either side of the panel. It was important to arrange these gages so that they indicated the displacement of the lower set of angles with respect to the upper set, and did not include the motion of the lower head.

Compression loads were applied in small, equal increments; and after each loading, permanent set readings were taken. The ultimate load carried by a panel was taken as the load beyond which the sheet continued to compress with no increase of force. In order to obtain uniform deflection of both sides of the panel, it was found necessary to locate the ring gage accurately along the reaction axis of the I-beam, panel system. No extensometer readings were attempted.

The procedure for the shear tests and the combined loading tests were the same. With no shear load, the appropriate compressive load was applied, and then the lower head of the machine was tightly clamped in position by means of set-screws between the uprights and the head. In the case of shear alone, the head was clamped as stated, with no compressive load. This was done so that the head could not twist about a horizontal axis perpendicular to its length when the shear load was applied. Thus no bending moment was introduced into the sheet by the shear loads.

The shear load was then applied by the strap gage described heretofore, and lateral deflection of the lower set of angles measured by another Ames dial gage. It was quite essential to locate this dial gage so that it indicated the deflection between the upper and lower ends of the sheet, and was in no way connected to the lower head of the machine. The shear load was applied so that there were no unreasonably large intervals between successive readings of either load or deflection. Care had to be taken to eliminate friction in the shear device before each reading, and to load the gage always in the same direction to obviate hysteresis effects.

Since it was necessary to clamp the lower head of the machine to the uprights, the lateral shear deflection would tend to induce a tension force into the sheet unless the panel were allowed vertical displacement. To compensate for this induced tension, the lower head was moved upward a pre-determined amount dependent upon the lateral deflection. The basis for this compensating deflection is given in Section V. At all times the lower end of the sheet was kept parallel to the upper.

As in the case of compression alone, for combined shear and compression the ultimate load carried by a particular panel was chosen as that value beyond which shear deflection occurred with no increase of force.

As will be shown from inspection of the resulting stress-strain curves, it was necessary to continue loading beyond the point where first the shear load decreased with an increase in displacement, and to continue applying load until the panel definitely would not support an increase in load.

V. DISCUSSION OF RESULTS

(a) Combined loading:

From inspection of the stress-strain curves of the panels under combined shear and compression, Figs. 9-12, and also from observation during the testing of the panels, it is apparent that failure occurs due to wave phenomena; that is, the sheet fails in compressive stress induced by the wave patterns. Hence this failing stress should be a continuous function of the initial compressive stress. Such a relation is demonstrated in Fig. 2-5.

In these figures, P_s/P_{s_o} is the ratio of the maximum shear load attained by each panel under combined loading to the shear load of the same panel under shear alone. Similarly, P_c/P_{c_o} is the ratio of the applied compressive load under combined loading to the ultimate load in compression alone. Each of these loads is the faired value obtained from the appropriate curve.

The shape of a curve faired through these points suggests that such a relationship should be closely approximate by an equation of the form:

$$\left(\frac{P_c}{P_{c_o}}\right)+\left(\frac{P_s}{P_{s_o}}\right)^n = 1 \qquad \text{Eq. 1}$$

where n is a factor to be determined analytically or experimentally. The experimental points were plotted on

log-log paper; the slope of the resulting straight line yielding values of n for each of the four cases investigated. Using these values of $\wedge n$, Eq. 1 was plotted on these figures. It can be seen that the agreement with experiment is quite good so that Eq. I does closely represent the conditions encountered in this problem.

It is very interesting to note that in all four cases the value of n, determined as indicated, was approximately the same, the range of slopes being from 3.90 to 4.10. Taking the average value of n, that is, 4.0, the resulting quartic parabola is plotted on Fig. 6, together with the experimental points for all the tests. Again there is good agreement with experimenta. Thus it can be said that for the thicknesses and length over width ratios tested the variation of shear and compressive loads may be represented by the equation:

$$\left(\frac{P_c}{P_{c_o}}\right) + \left(\frac{P_s}{P_{s_o}}\right)^4 = 1 \qquad \text{Eq. 2}$$

Although insufficient data are at hand to justify extension of Eq. 2 beyond $t = 0.022"$ to $0.032"$ and $a/b = 2$ to 3, within that range Eq. 2 should hold closely for thin, flat, unstiffened panels.

Eq. 1 has been applied to other similar cases by various investigators. Wagner gives this expression with $n = 2$ for buckling of flat strips under combined shear and

compression (Ref. 4). Bridget, et al, also used this formula with $n = 3$ for critical stresses in unstiffened circular cylinders under this type of loading (Ref. 5). The shape of the resulting curve in each case is what would be expected intuitively; since of necessity the curve must be continuous and have a zero slope at $P_c/P_{c_o} = 1$, $P_s/P_{s_o} = 0$, and should have a finite negative slope at $P_c/P_{c_o} = 0$, $P_s/P_{s_o} = 1$ due to the stabilizing effect of negative compression (i.e., tension) in buckling problems.

(b) Wave forms

Upon first buckling in compression alone the panels assumed a square wave form; that is, with the half wavelength equal to the width, with one exception shown in Photo. 1. In this case of $t = 0.0215"$, $a/b = 3$, five half-waves were formed initially. Upon increasing the compressive load beyond the critical value, in each instance additional waves appeared along the edges, as many as nine or eleven waves on each side being evident before failure. Failure generally occurred along the edge after the local wave form had become excessively deep.

In the cases of shear and combined loading the axis of the initial shear wave was approximately at 45^o with the shear direction running from each tension corner. Slightly greater loads changed that axis to one between

tension corners for both a/b ratios. This shift becomes most obvious in Fig. 10 for the panels under large compressive loads. When approaching the ultimate loads, the continuous alteration of wave pattern can be seen most clearly in Fig. 10 for panels under small compressive loads. Photos. 2 and 3 also demonstrate this phenomenon.

(c) Compression Correction

As has been mentioned previously, it became necessary to correct the compression deflection of the panel under combined loads for the tensile force induced in the sheet by lateral shear displacement of the lower end of the sheet. The curve used for this purpose was calculated as follows: a particular shear deflection corresponds to an elongation of each element of the sheet if the distance between the ends of the sheet were constrained to remain constant. This extension was converted to a stress, and then to a load, by the usual stress-strain relations, and the observed compressive deflection of the panel corresponding to that calculated load was imposed upon the sheet to bring the ends closer. Curves of this correction for each series of panels are given in the Appendix, page 36.

(d) Discussion of Curves

In Fig. 7 the load-strain curves for each of the panels tested in pure compression are drawn, using applied load as ordinates and unit elongation as abscissa. Obtaining the faired values of the failure loads, and comparing with values derived from Dr. E. E. Sechler's experimental work on effective width (Ref. 2), the following table is obtained:

Table I

t"	b "	λ	$P^{\#}_{exp.}$	$P^{\#}_{Sech.}$	$\eta \left(=\frac{P_{exp.}}{P_{Sech.}}\right)$
0.0220	9.0	0.0396	835	540	1.55
0.0320	9.0	0.0581	1750	1075	1.62
0.0220	6.0	0.0595	825	500	1.64
0.0320	6.0	0.0871	1650	1010	1.63

In calculating $\lambda \left(=\frac{t}{b}\sqrt{\frac{E}{\text{yield}}}\right)$ the yield stress in compression was assumed to be 38,000#/sq.in. and E was taken as 10.4×10^6#/sq.in.

In Dr. Sechler's tests the panels were simply supported by V-grooves on all four sides. In this work, the panels were built in at each end, and given a line support along the other two edges by the split tubes as stated. Indications are that these tubes furnish an edge-fixity coefficient greater than that of V-grooves; i.e., greater

than 1. This would be expected since tube restraint supplies an edge-moment along the sheet when the wave pattern is such that bending deflection in the plane of the sheet is not uniform along the edge.

In Dr. Sechler's work the strips adjacent to the edge supports carried the greater portion of load after buckling, and the center elements of the sheet carried little more than the critical load. However, in the present experiments the sheet close to all four sides carried load, and only a small center portion of the sheet could not sustain appreciable loads above the critical. Thus with the edge conditions used, the "effective width," and thereby the ultimate load, of the panel is increased by the ratio η . For the range of sheet sizes and thicknesses tested, η may be taken as 1.63, the mode of the values in Table I preceding.

The load-strain curves for shear alone are given in Fig. 8. In this case again, the ordinates are applied load, and the abscissa are lateral displacements per unit length of panel. Obtaining the maximum loads, for this case the ratio of ultimate loads for the two thicknesses is 1.97 for a/b = 3, and 1.99 for a/b = 2. The variation of maximum shear loads with a/b is 1.62 for t = 0.022" and 1.63 for t = 0.032", the lower a/b ratio resulting in the higher ultimate load. Insufficient data are available

from these tests to determine the variation of ultimate shear load with both t and a/b ratio.

References, graphical results, index of tests, and calibration curves are given in the following sections.

VI. REFERENCES

1. Schapitz, E.: "Contributions to the Theory of Incomplete Tension Bay." TM 831, N.A.C.A.

2. Sechler, E. E.: "Stress Distribution in Stiffened Panels under Compression." Journ. Aero. Sciences, June 1937, p. 320. (See also GALCIT Pub. 27, 1933.)

3. Timoshenko, S.: "Theory of Elastic Stability." McGraw-Hill, 1936.

4. Wagner, H.: "Structures of Thin Sheet Metal." TM 490, N.A.C.A.

5. Bridget, F.J., Jerome, C.C., and Wasseler, A.B.: "Some New Experiments on Buckling of Thin-Wall Constructions." Trans. A.S.M.E., Vol. 56, No. 8, 1934, pp. 569-578.

VII. GRAPHICAL RESULTS

Explanation of symbols on Fig. 1:

(a) Upper head

(b) Lower head

(c) Ring gage for compression loading

(d) Adjusting nut for ring gage

(e) Strap gage for shear loading

(f) Strap gage support

(g) Adjusting lead-screw for strap gage

(h) Deflection gage for compression

(i) Deflection gage for shear

(k) Rollers for shear deflection

(l) Roller bearing for lower angle restraint

(m) Lower angle

(n) Upper angle

(o) Tube edge supports

(p) Tube turnbuckles

(q) Lower head clamps

(r) Test panel

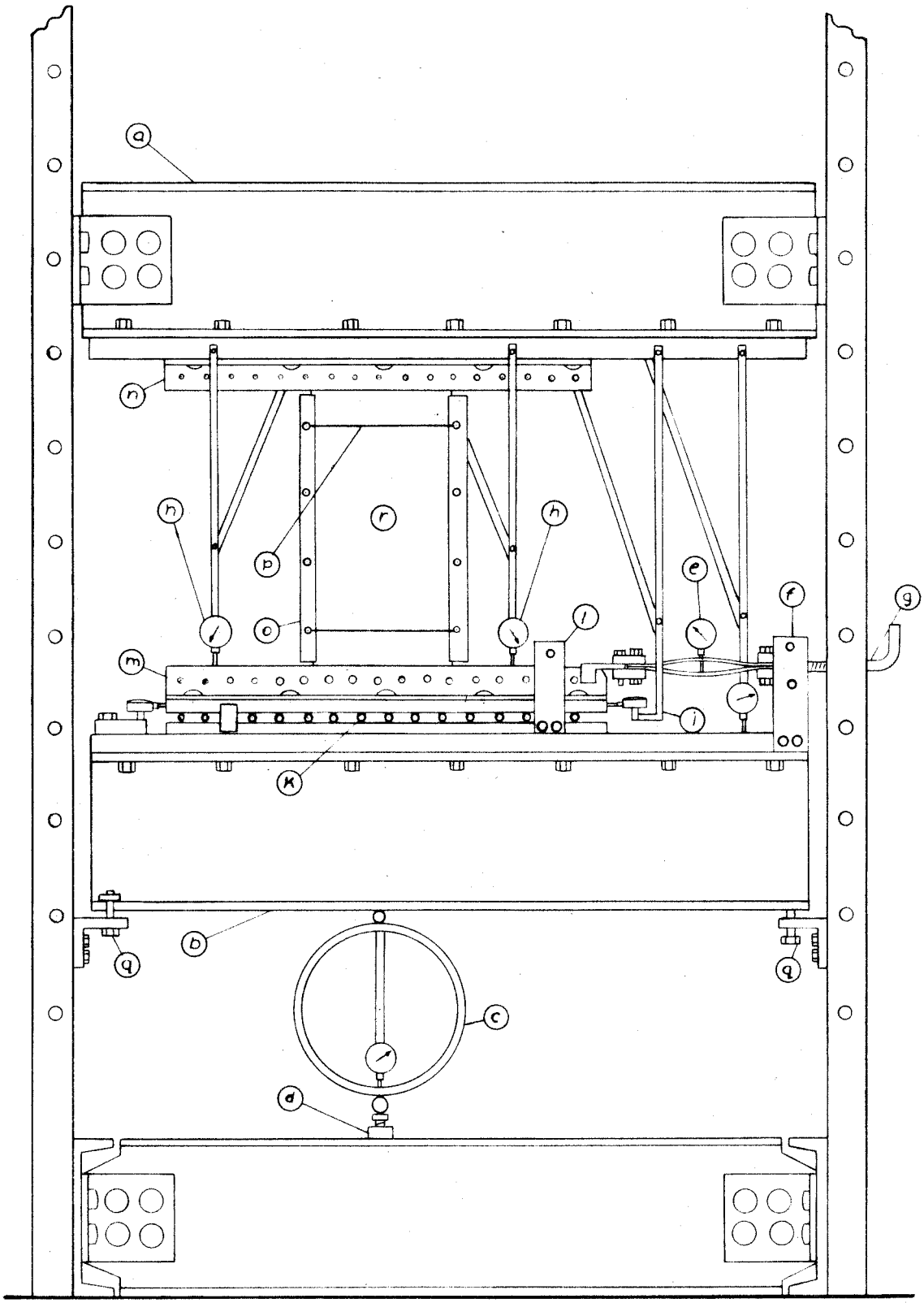

FIG. 1

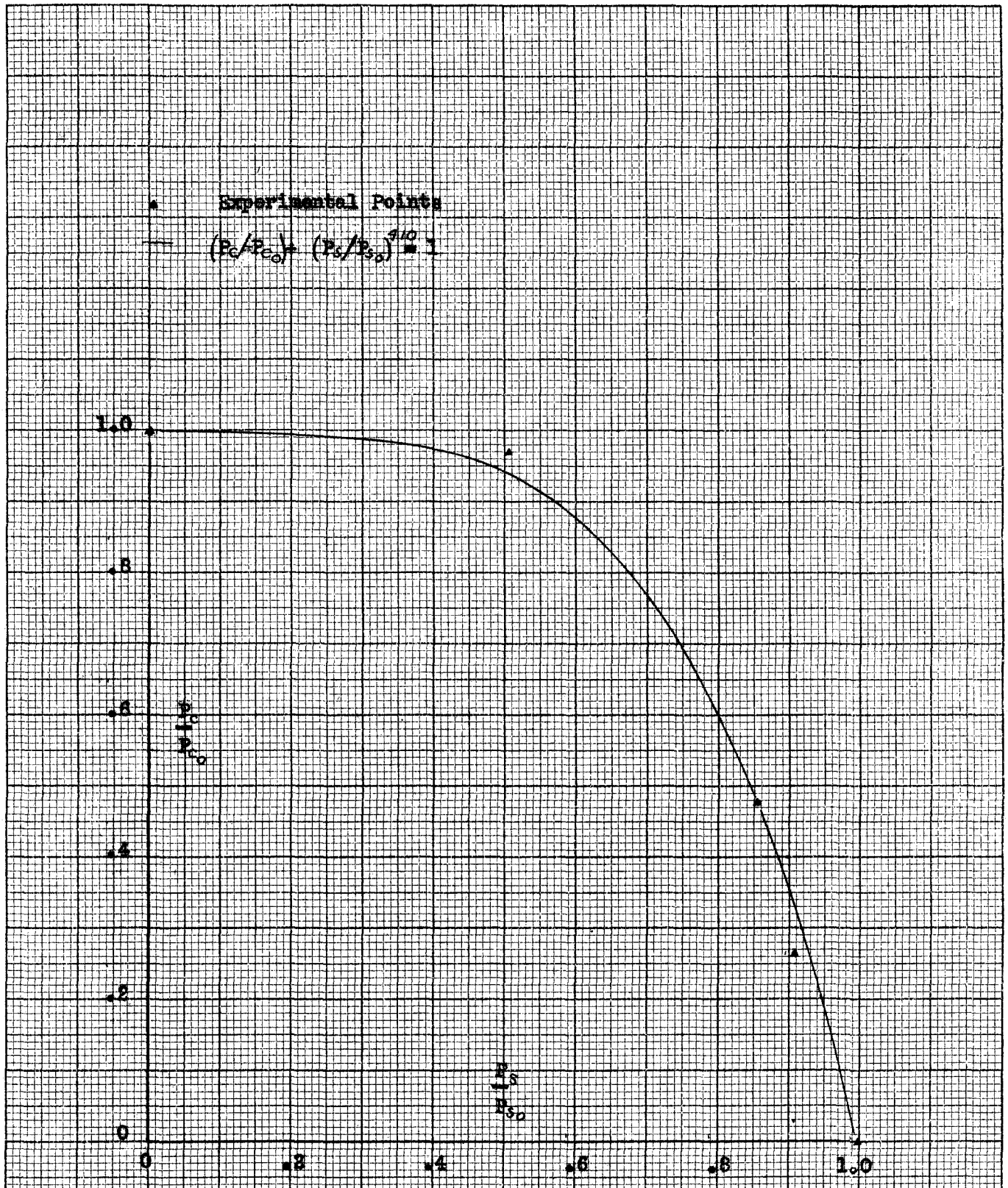

Fig. 2 - Variation of Combined Loads for a/b = 2, t = 0.022" (nominal)

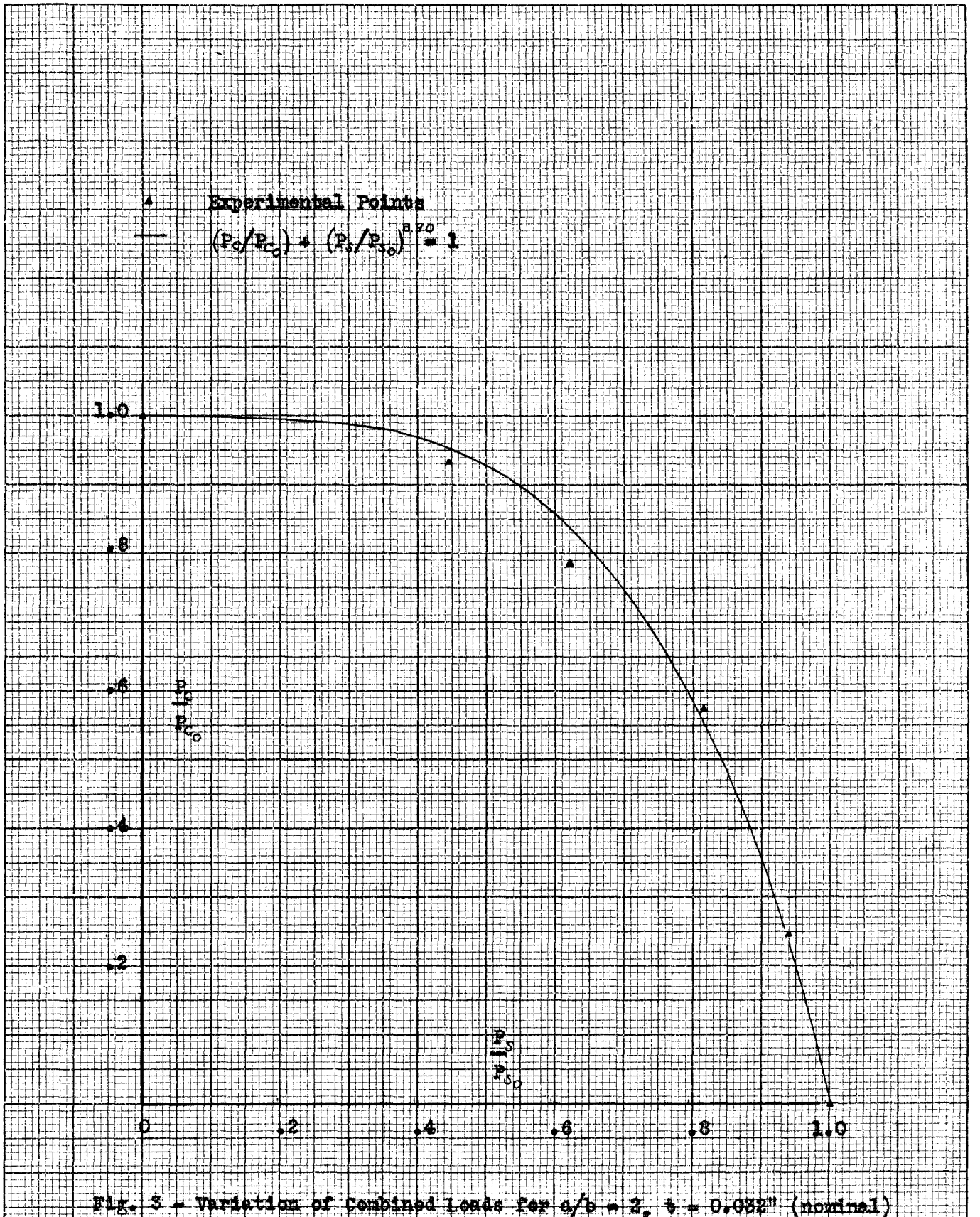

Fig. 3 - Variation of Combined Loads for a/b = 2, t = 0.082" (nominal)

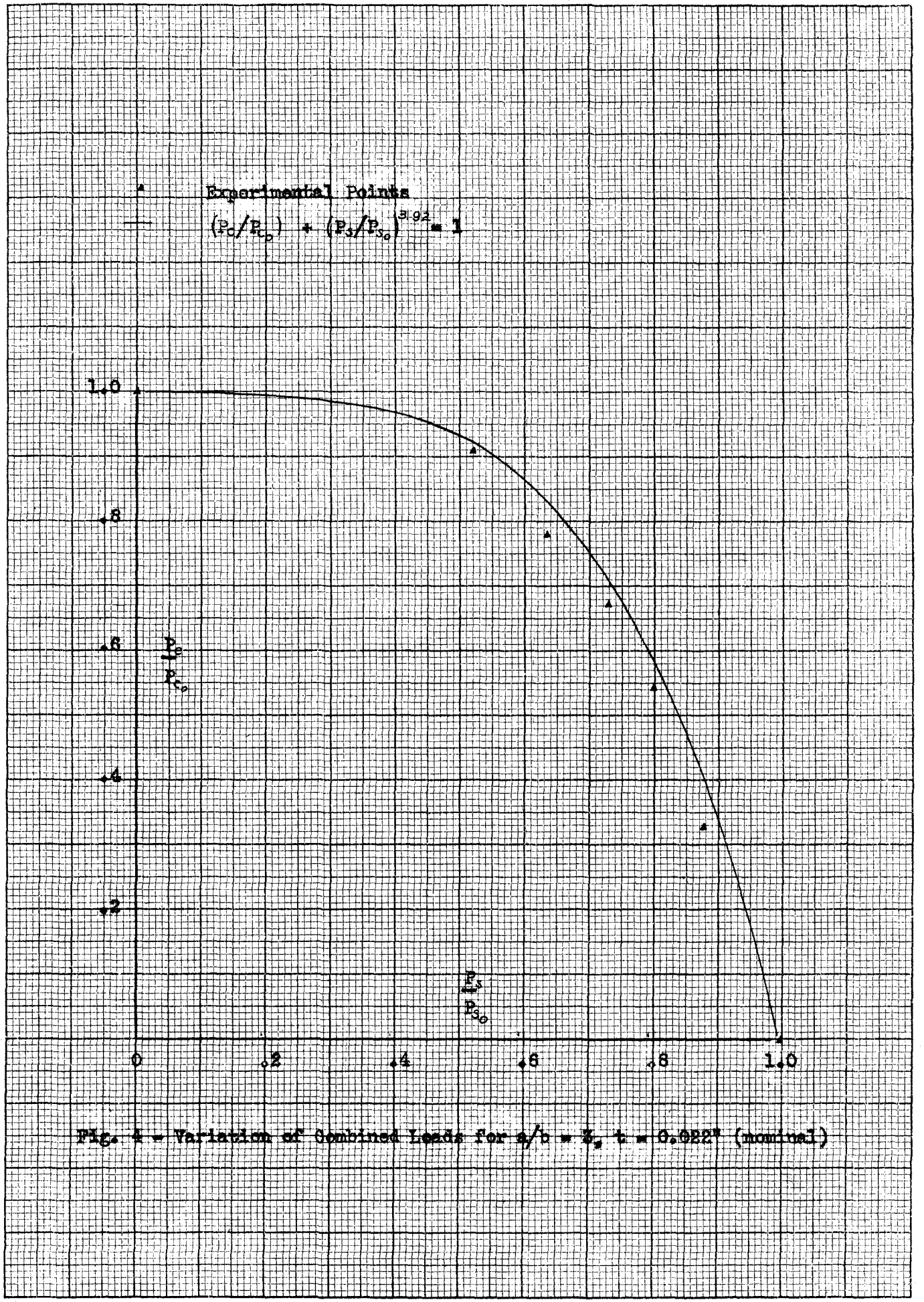

Fig. 4 - Variation of Combined Loads for a/b = ½, t = 0.022" (nominal)

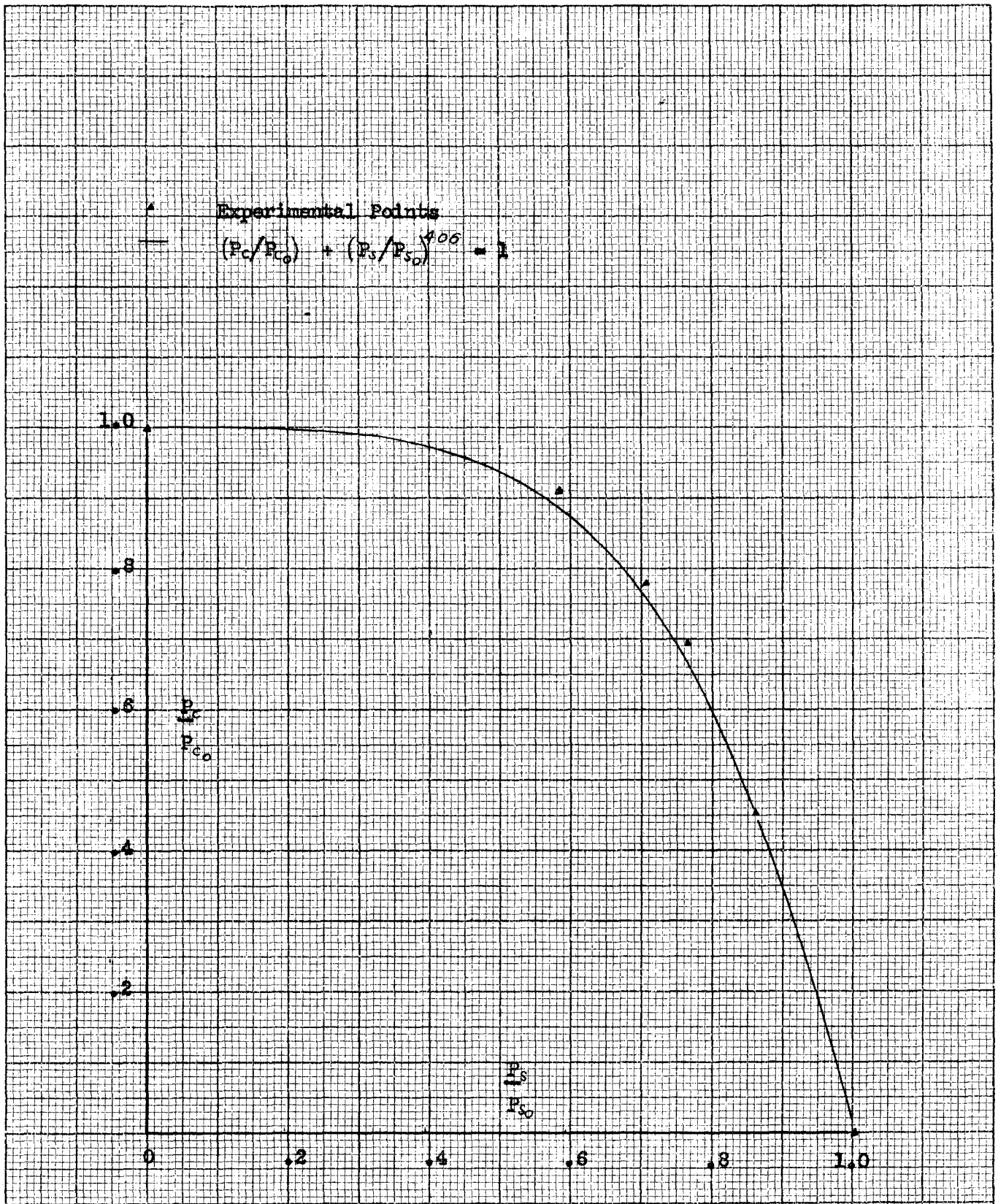

Fig. 5 - Variation of Combined Loads for a/b = 3, t = 0.052" (nominal)

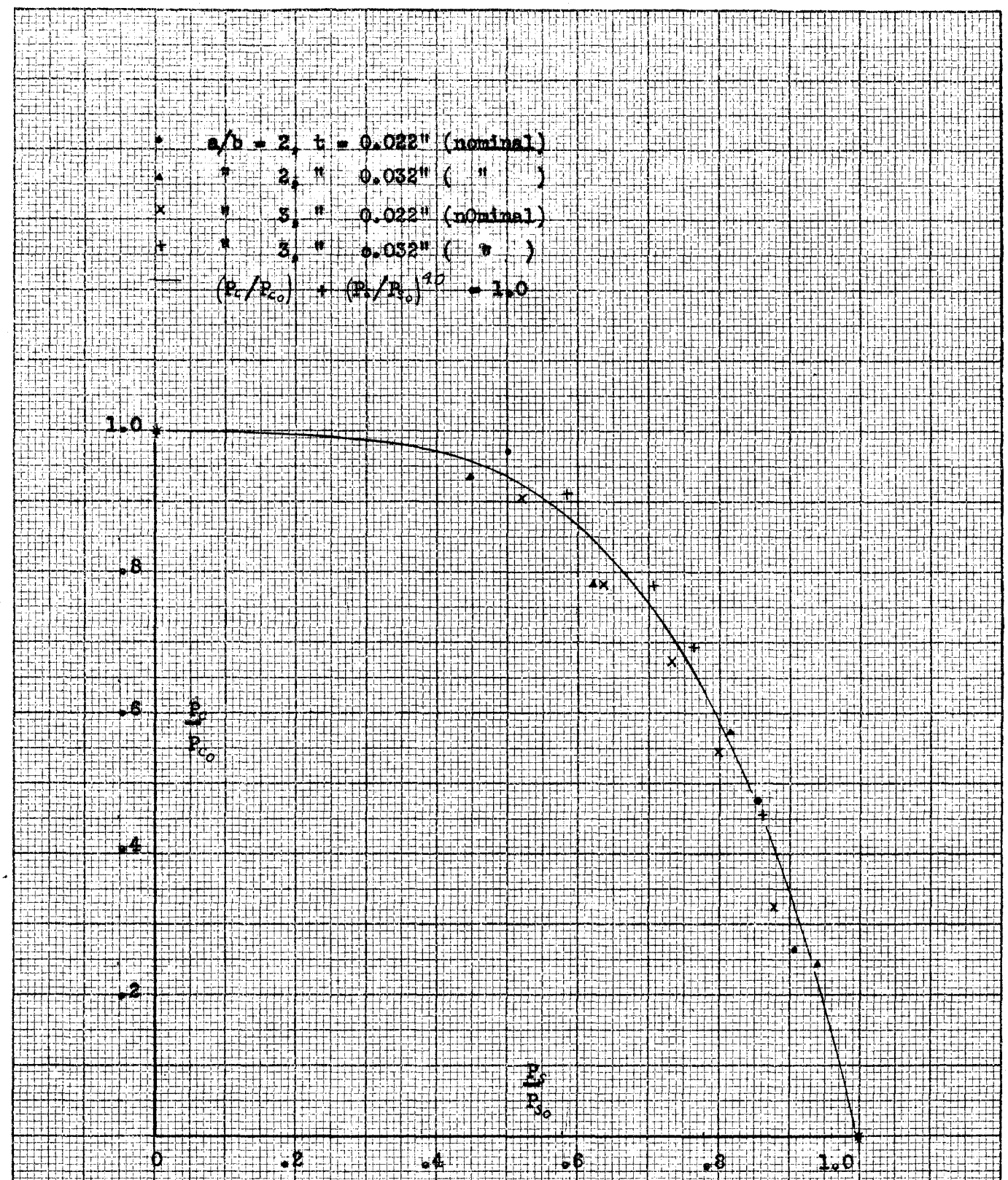

Fig. 6 - Variation of Combined Loads, Composite Curve

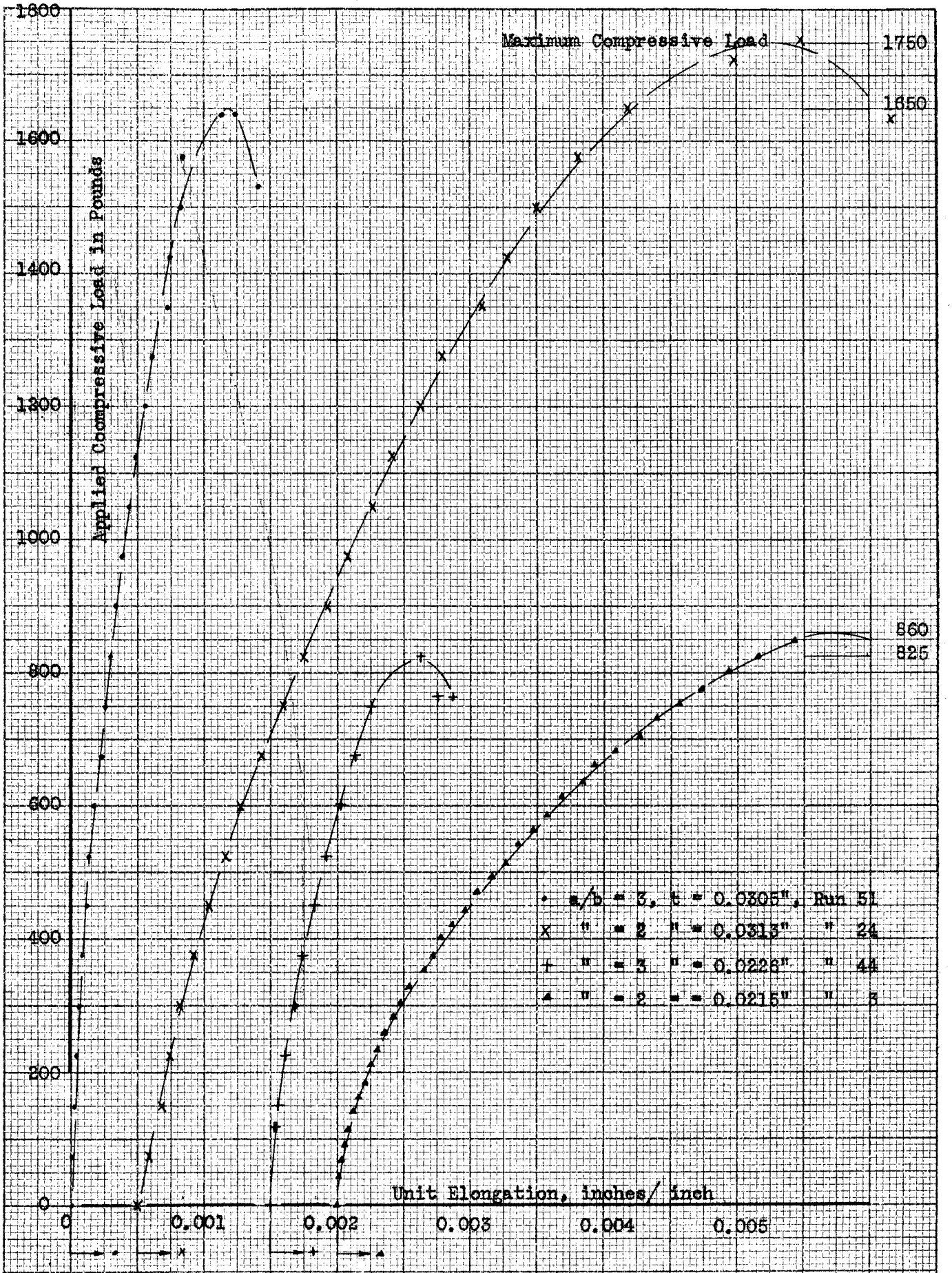

Fig. 7 - Load-Strain Curves for Compression Alone with Various Thicknesses

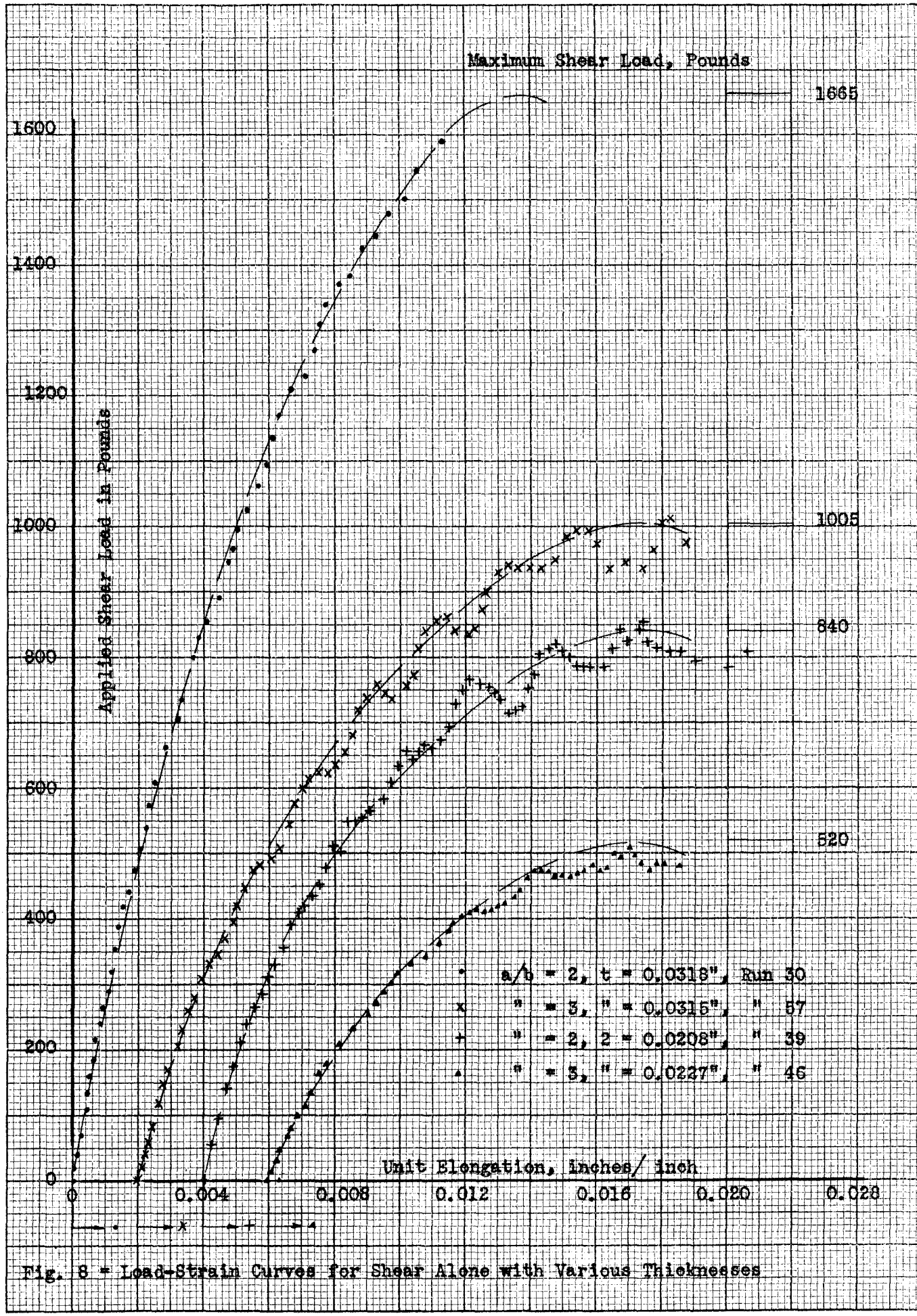

Fig. 8 - Load-Strain Curves for Shear Alone with Various Thicknesses

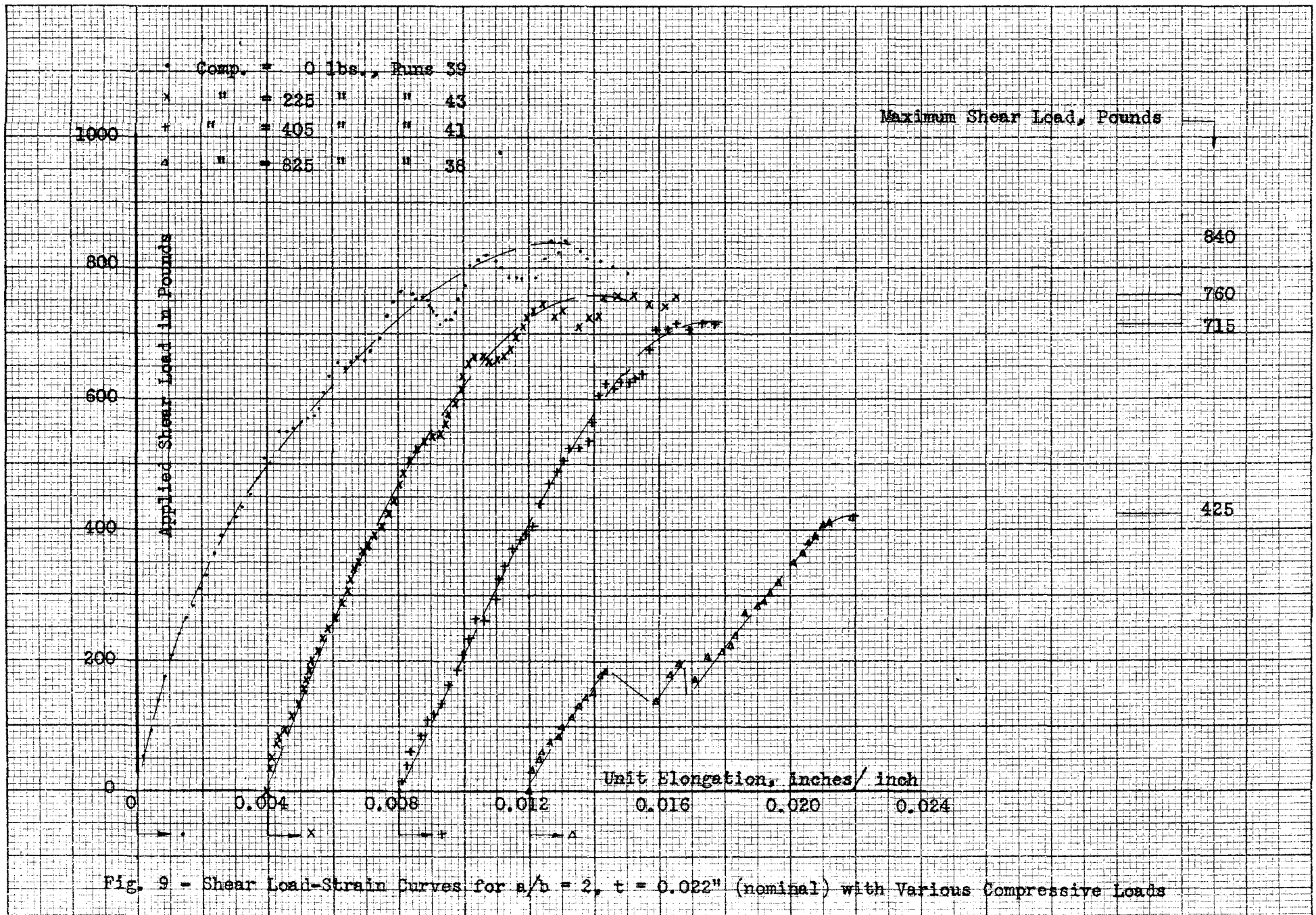

Fig. 9 - Shear Load-Strain Curves for a/b = 2, t = 0.022" (nominal) with Various Compressive Loads

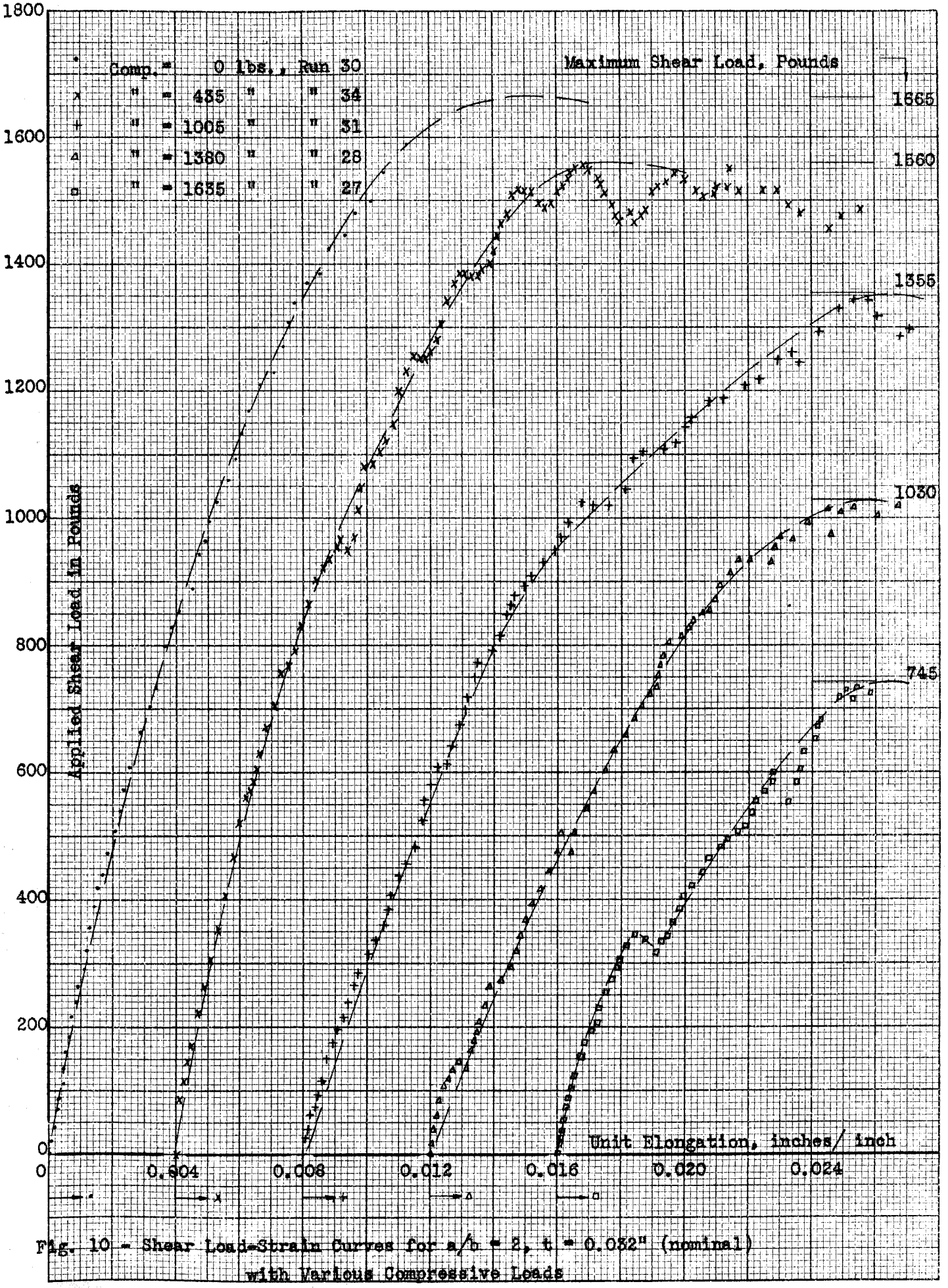

Fig. 10 - Shear Load-Strain Curves for a/b = 2, t = 0.032" (nominal) with Various Compressive Loads

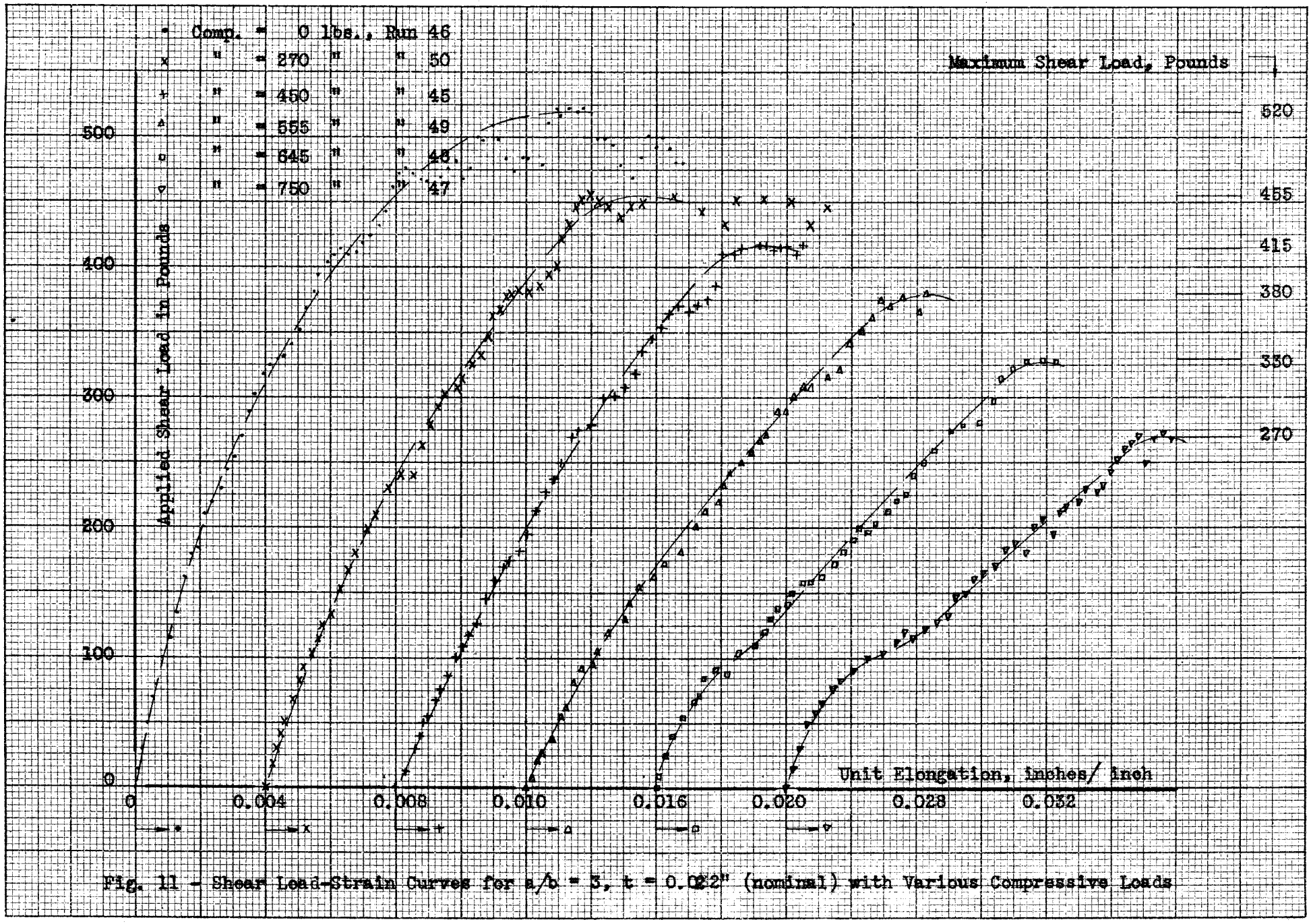

Fig. 11 - Shear Load-Strain Curves for a/b = 3, t = 0.022" (nominal) with Various Compressive Loads

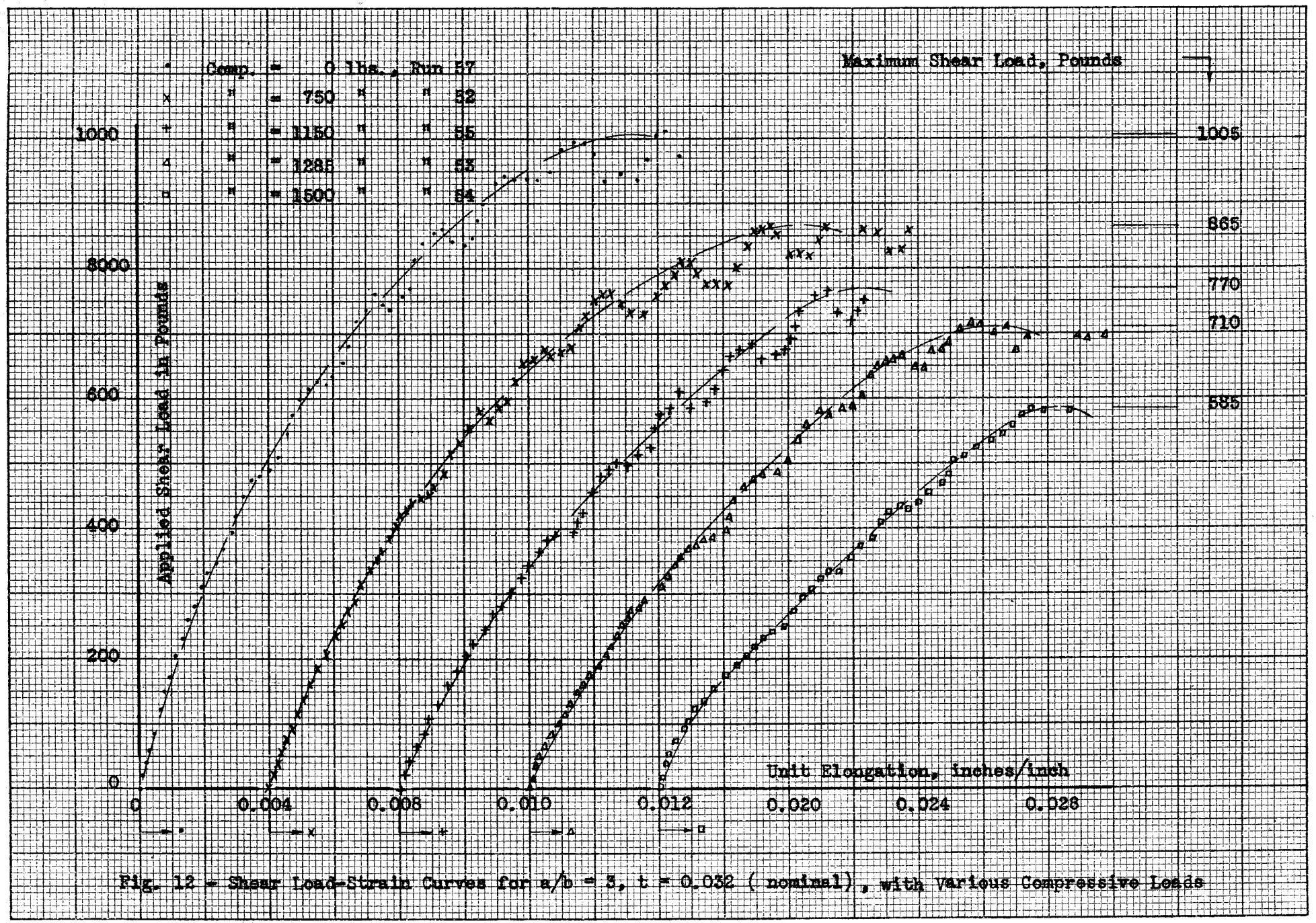

Fig. 12 - Shear Load-Strain Curves for a/b = 3, t = 0.032 (nominal), with Various Compressive Loads

VIII. APPENDIX

Index of Tests

Fig. 1a - Calibration Curves for Ring Gages

Fig. 2a - Calibration Curves for Strap gage

Fig. 3a - Compression Correction Curves

Photographs.

Index of Runs

Run No.	a/b Ratio	t inches	P_c Comp. Load pounds	Max.P_s Shear Load pounds	P_c/P_{c_o}	P_s/P_{s_o}
3	2	0.0215	835	0	1.000	0.000
38	2	0.0210	825	425	0.986	0.506
39	2	0.0208	0	840	0.000	1.000
41	2	0.0212	405	715	0.485	0.851
43	2	0.0211	225	760	0.269	0.905
24	2	0.0313	1750	0	1.000	0.000
27	2	0.0312	1635	745	0.931	0.447
28	2	0.0310	1380	1030	0.786	0.620
30	2	0.0318	0	1665	0.000	1.000
31	2	0.0308	1005	1355	0.573	0.815
34	2	0.0316	435	1560	0.248	0.938
44	3	0.0226	825	0	1.000	0.000
45	3	0.0228	450	415	0.545	0.799
46	3	0.0227	0	520	0.000	1.000
47	3	0.0206	750	270	0.909	0.520
48	3	0.0210	645	330	0.781	0.635
49	3	0.0210	555	380	0.672	0.730
50	3	0.0210	270	455	0.327	0.875
51	3	0.0305	1650	0	1.000	0.000
52	3	0.0310	750	865	0.454	0.860
53	3	0.0312	1285	710	0.780	0.706
54	3	0.0312	1500	585	0.910	0.582
55	3	0.0311	1150	770	0.697	0.766
57	3	0.0315	0	1005	0.000	1.000

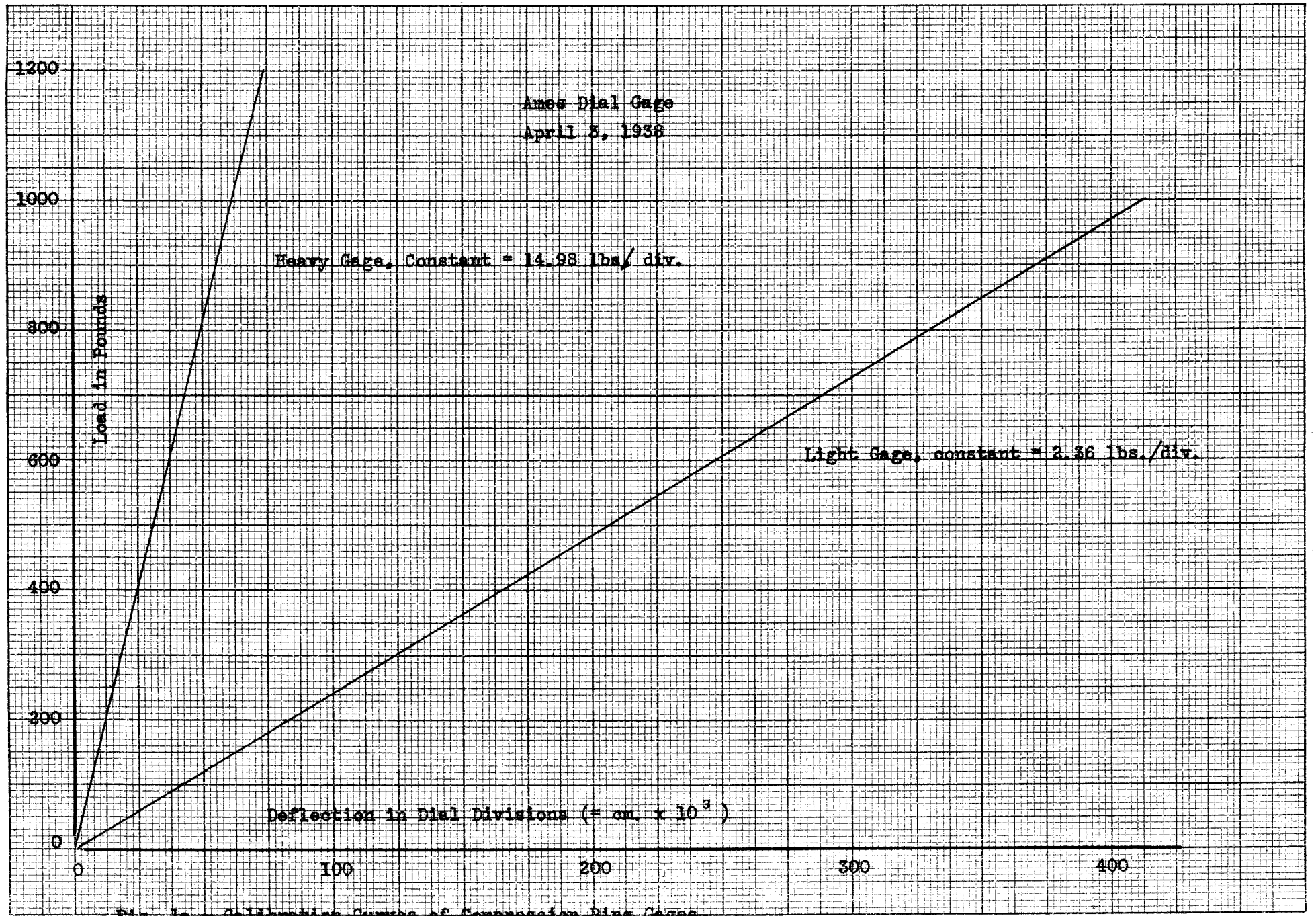

Fig. 1a - Calibration Curves of Compression Ring Gages

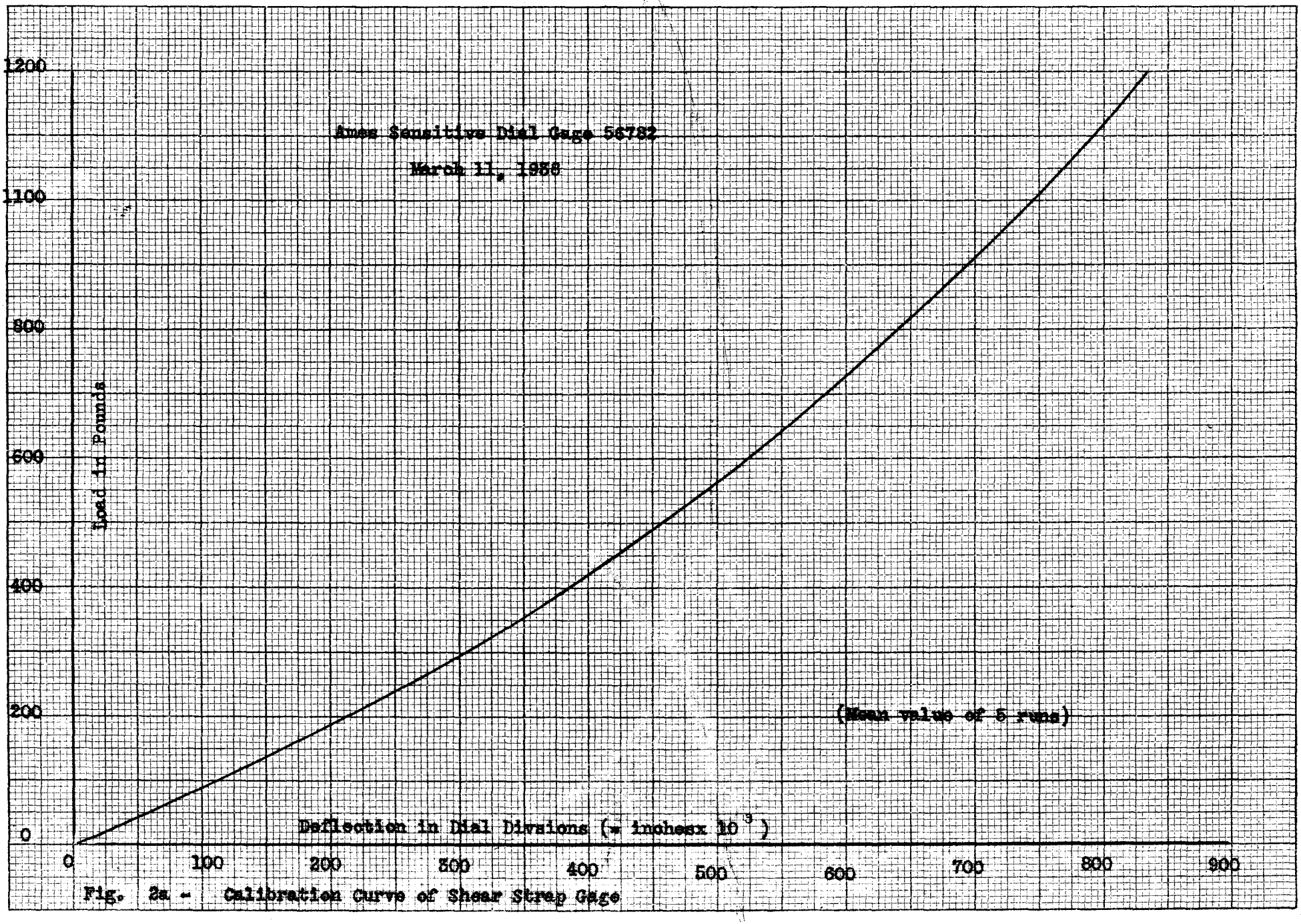

Fig. 2a - Calibration Curve of Shear Strap Gage

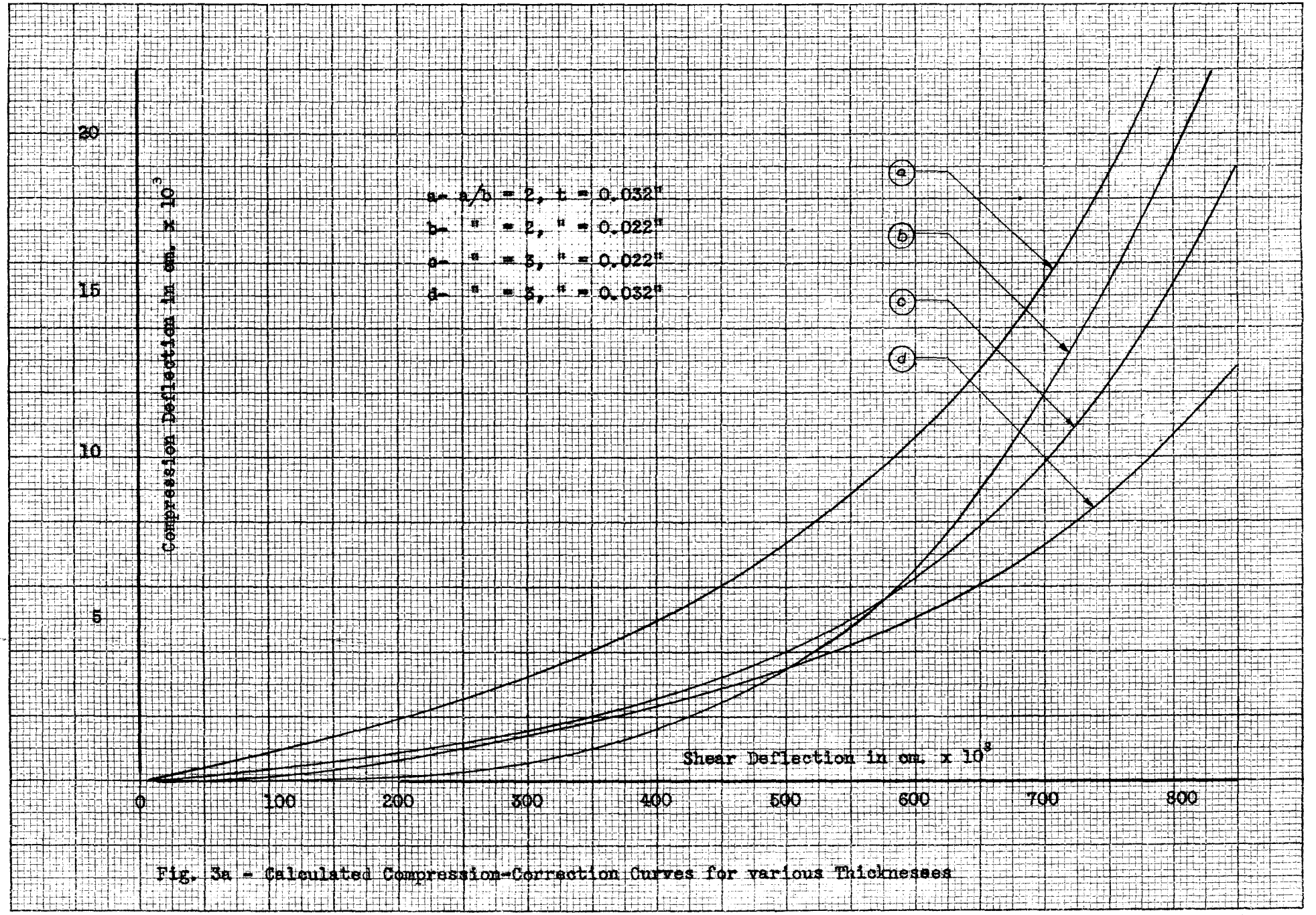

Fig. 3a - Calculated Compression-Correction Curves for various Thicknesses

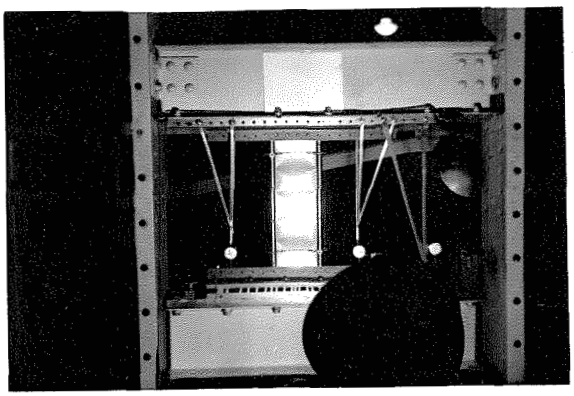

Fig. 1 - Initial
Compression Waves

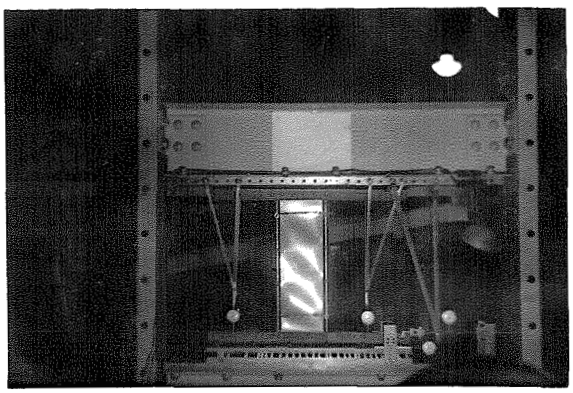

Fig. 2 - Initial
Combined Waves

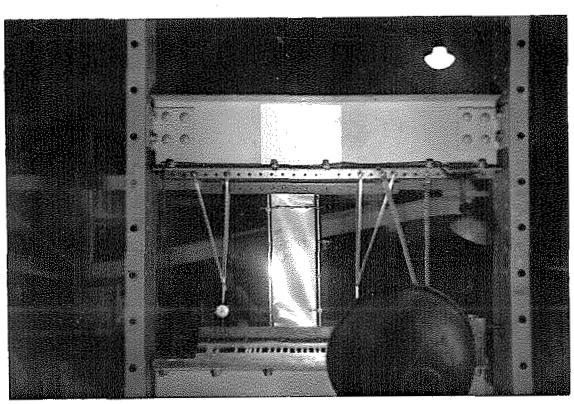

Fig. 3 - Final
Combined Waves

$a/b = 3, \quad t = 0.0215"$

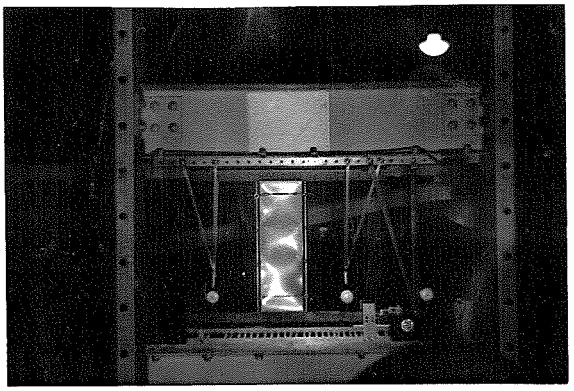

Fig. 1 - Initial
Compression Waves
a/b = 3, t = 0.0315"

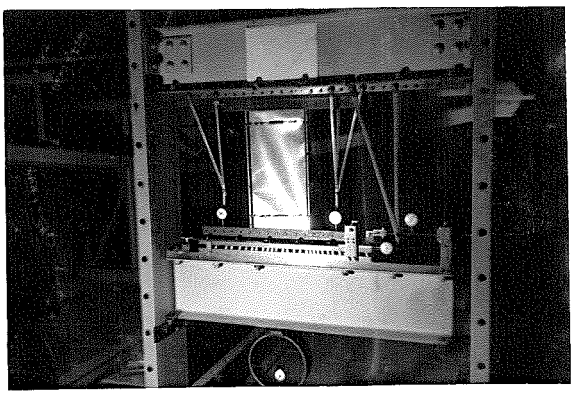

Fig. 5 - Final
Combined Waves
a/b = 2, t = 0.0315"

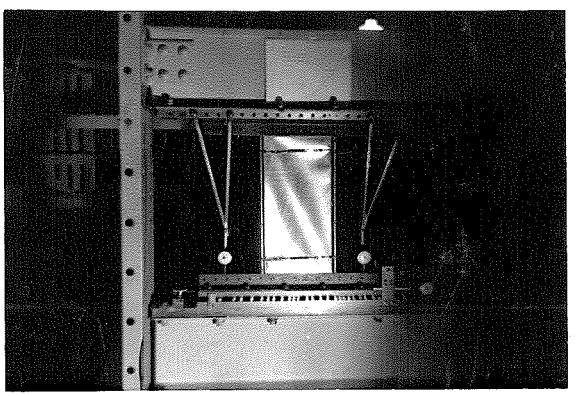

Fig. 5 - Final
Combined Waves
a/b = 2, t = 0.0215"